NASA TECHNICAL MEMORANDUM

NASA TM X-71698
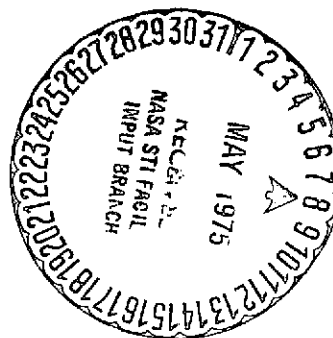
NASA TM X-71698

MAGNETIZATION AND MAGNETIC SUSCEPTIBILITY OF DyH$_3$

by D. J. Flood
Lewis Research Center
Cleveland, Ohio 44135

MAGNETIZATION AND MAGNETIC SUSCEPTIBILITY OF DyH$_3$

by D. J. Flood

Lewis Research Center

ABSTRACT

The magnetization and differential magnetic susceptibility of powdered samples of DyH$_3$ have been measured at 4.2 K in applied magnetic fields ranging to 9 Teslas. The differential magnetic susceptibility has also been studied in zero applied field as a function of temperature. The magnetization data are described by an equation of the form $M = \left[aB/(1 + bB)\right] + cB$. The ratio a/b is a measure of the saturation magnetization and gives an effective moment of 5.12 Bohr magnetons per ion. The zero field susceptibility exhibits a maximum at $T = 3.45$ K, and an inflection point near 2.85 K. The susceptibility at 4.2 K has a $1/B^2$ dependence on the applied magnetic field for $B \gtrsim 0.3$ Teslas.

Introduction

The magnetic properties of rare earth materials are extremely varied and numerous, and have been the subject of many investigations. (See refs. 1 and 2 for excellent reviews of some of the fundamental aspects of rare earth magnetism.) The so-called heavy rare earth ions, listed in table I, have total angular momenta J produced by a strong spin-orbit coupling of L and S, the orbital and spin angular momenta, respectively. J values are large in the "heavy" rare earths because Hund's rules call for $J = L + S$, rather than $J = L - S$ as in the "light" RE's. Ground state S and L are determined by applying Hund's rules to the electrons in the 4f shell. g_L is the Laudé g factor. These materials exhibit a surprising degree of free-ion magnetic behavior in the solid state, primarily because the 4f shell remains highly localized, and is often relatively unaffected by the crystalline environment. Magnetic dipole interactions in the rare earths, for example, are very weak, causing ordering effects only for temperatures in the neighborhood of 1 K. Exchange interactions and crystal fields determine the magnetic behavior, many times with one or the other dominant, and many times with competing effects, but almost always with effects that are important only at low temperatures (10 to 100 K). (The energy differences between the various J values in the rare earths correspond typically to 1000 K or more due to the large spin-orbit coupling.)

The heavy rare earths crystallize in hexagonal close-packed structures (see fig. 1) with c/a ratios varying between 1.57 and 1.59, slightly below the ideal value of 1.63. Adding hydrogen to the metal changes the lattice parameters, resulting in a c/a ratio of 1.801 for DyH_3 (ref. 3). The increase in c/a ratio occurs primarily because of distension along the c axis, although both c and a are larger in the trihydride than the pure metal. The magnetic structure found in Dy metal in the temperature range 85 to 179 K consists of a net moment of constant amplitude located in the basal plane perpendicular to the c axis. The direction of the net moment varies from one crystallographic

plane to the next with a definite spatial periodicity, producing a magnetically ordered state with no net moment. In this range Dy is antiferromagnetic. Below 85 K, the moments all line up in one direction throughout the crystal, producing a ferromagnetic state. There is not, in either case, a net moment along the c axis. Kubota and Wallace (ref. 4) reported the complete disappearance of any magnetic ordering in $DyH_{2.92}$, $DyH_{2.93}$, and $DyH_{2.97}$ in the range ~3 to 300 K. Their explanation is that hydrogen exists in the lattice as an anion, acquiring electrons from the conduction band of the metal. Since the primary exchange interaction producing the original magnetic order is via the conduction electrons, loss of them leaves only the exchange interaction involving the 4f electrons, which is very weak. Hence ordering can occur only at lower temperatures, and will most likely be antiferromagnetic.

II. Experimental Techniques

The investigation was made on commercially prepared samples of DyH_3. X-ray analysis by the supplier showed no traces of other phases of the hydrides, nor of elemental Dy. Magnetization data were obtained by sweeping the dc magnetic field and integrating the induced difference voltage from two search coils, one of which contained the sample. Differential susceptibility measurements, using standard field-modulation techniques, were made to study χ_{diff} both as a function of field and as a function of temperature. Temperatures were measured using standard 1/8 watt, 100 ohm carbon resistors calibrated against the vapor pressure of liquid helium. Field modulation measurements were made in a 10.5 Tesla (1 T = 10 k gauss), 2.5 in. diameter bore (6.35 cm) superconductive solenoid, and magnetization measurements were made in a 7.5 Tesla, water-cooled 4 in. diameter (10.2 cm) bore copper solenoid.

4

III. Results and Discussion

The dc magnetization at 4.18 and 3.97 K is shown as a function of applied field in figure 2. The solid line is a plot of the function

$$M = \frac{aB}{1 + bB} + cB \tag{1}$$

using $a = 94.0 \times 10^4$ (amp/m)/T, $b = 1.85$ T^{-1}, and $c = 11.5 \times 10^3$ (amp/m)/T, with B in Teslas. The curve generated using the above values fits the experimental data to within 1.5 percent over the range 1.0 to 7.4 Tesla. Below 1.0 Tesla the agreement gets increasingly worse, reaching as much as 16 percent at 0.13 Tesla. No one set of (abc) values provided a fit over the whole range that was within experimental accuracy at all points, which means that eq. (1) is not an entirely suitable approximation for all fields. Since it does describe the moderate to high field behavior very well, however, we shall use it to calculate the saturation magnetization. From eq. (1)

$$\lim_{B \to \infty} (M(B) - cB) = M_{sat} = \lim_{B \to \infty} \frac{aB}{1 + bB} = a/b \tag{2}$$

From the values given for a and b,

$$M_{sat} = 5.08 \times 10^5 \text{ amp/m} \tag{3}$$

However, for wide multiplet splitting compared to kT,

$$M_{sat} = N\mu_B(g_p J') \tag{4}$$

where N is the number of magnetic ions per m^3, μ_B is the Bohr magneton, g_p is the spectroscopic splitting factor appropriate for a powder, and J' is the effective spin of the ground state. For the sample used,

$N = 10.7 \pm 0.4 \times 10^{27}$ ions/m^3 and

$$(g_P J') = 5.12 \pm 0.18 \tag{5}$$

is the effective saturation magnetic moment per ion. The above result is considerably below the free ion value of 10, and is an indication of the effect of the crystal field on the magnetic ground state. From the discussion on structure in the introduction, it is not unreasonable to expect that DyH$_3$ will be extremely anisotropic since $c/a \sim 1.8$. Such would be the case if the ground state were a Kramers doublet with $J_z = \pm 15/2$. In that situation $g_P = g_L \langle J_z \rangle$, where g_L is the free-ion Landé g-factor, and $J' = 1/2$. Hence

$$(g_P J') = \frac{4}{3} \left(\frac{15}{2} \right) \times \frac{1}{2} = 5 \tag{6}$$

which agrees, within the indicated uncertainty, with the result in eq. (5).

Figure 3 is a plot of the differential susceptibility (in arbitrary units) as a function of temperature in zero applied magnetic field. A rather broad maximum occurs in χ_{diff} near $T = 3.45$ K, with $x_p(0)/x_p(T_N) \simeq 2/3$ indicating antiferromagnetic ordering below that temperature. The local minimum in χ_{diff} near $T = 2.85$ K is unusual and as yet unexplained. It may possibly indicate the actual Neél temperature T_N, which is always lower than the temperature for which χ is a maximum, although normally only an inflection is observed in χ versus T at T_N ($d\chi/dT$ is a maximum at T_N). Measurements of the specific heat or magnetic entropy should help provide an understanding of the anomaly. (It may have its origin in the presence of a magnetic impurity which somehow escaped detection when the sample purity was analyzed. All of the rare earth sesquioxides (R_2O_3) order antiferromagnetically below 4.2 K. It is not likely to be Dy$_2$O$_3$, however, since $T_N = 1.6$ K for that compound.)

The dependence of χ_{diff} on applied magnetic field is shown in figure 4 for $T = 4.2$ K. The solid curve is a plot of the equation

$$\frac{dM}{dB} = \frac{a'}{(1 + b'B)^2} + c' \tag{7}$$

obtained by differentiating eq. (1). The parameters (a'b'c') indicated in the figure have been chosen to fit eq. (7) to the experimental data with an error less than 1 percent over the range from 0.884 to 65.2 Tesla. At 0.576 Tesla the value given by eq. (7) is 3.5 percent too low. It was not possible to get reliable data in the range below about 0.5 Tesla, except for the zero field point, with the superconducting magnet because of its remnant field. The dc measurements indicate, however, that dM/dB is constant up to about 0.04 Tesla, and then begins to decrease as B increases. This kind of behavior in the paramagnetic region is indicative of interactions between the magnetic moments in the solid. The strong dependence of χ_{diff} on B at low fields, and the approach to a constant value at high fields lends support to the contention that the 16-fold degeneracy of the Dy^{+3} ions has been removed by crystal fields. The finite value of χ at high fields (the c' term in (7)) results from a van Vleck paramagnetism, which in turn reflects the presence of unfilled energy levels near the ground state, causing a perturbation of the ground state wave function.

IV. Conclusion

Results from differential susceptibility measurements on DyH_3 indicate that the compound orders antiferromagnetically below 3.45 K, and that χ_{diff} varies as $1/B^2$ for $B \gtrsim 0.3$ Tesla. A non-zero value for χ_{diff} in the high-field region is indicative of van Vleck paramagnetism. Magnetization measurements yield a saturation magnetic moment of 5.12 ± 0.18 Bohr magnetons per ion, far below the free-ion value of 10 μ_B. The results are consistent with the assumption that the magnetic ground state in DyH_3 is a Kramer's doublet with $J_z = \pm15/2$, and that other levels from the original $J = 15/2$ multiplet, which has been split by the crystal fields, lie near enough above the ground state to perturb it slightly.

References

1. Rhyne, James J.; and McGuire, Thomas R.: Magnetism of Rare-Earth Elements, Alloys, and Compounds. IEEE Trans. Magnetics, vol. MAG-8, no. 1, Mar. 1972, pp. 105-130.

2. Cooper, B. R.: Orbital Effects in Rare Earth Magnetism. Critical Reviews in Solid State Sciences, vol. 3, no. 1, Mar. 1972, pp. 83-129.

3. Pebler, A.; and Wallace, W. E.: Crystal Structures of Some Lanthanide Hydrides. J. Phys. Chem., vol. 66, no. 1, Jan. 1962, pp. 148-151.

4. Kubota, Yoshio; and Wallace, W. E.: Magnetic Characteristics of Dysprosium, Erbium, and Thulium Hydrides. J. Chem. Phys., vol. 39, no. 5, Sept. 1963, pp. 1285-1288.

Table I

Metal	Config-uration	L	S	J	g_L
Gd^{3+}	$4f^7$	0	7/2	7/2	2
Tb^{3+}	$4f^8$	3	3	6	3/2
Dy^{3+}	$4f^9$	5	5/2	15/2	4/3
Ho^{3+}	$4f^{10}$	6	2	8	5/4
Er^{3+}	$4f^{11}$	6	3/2	15/2	6/5
TM^{3+}	$4f^{12}$	5	1	6	7/6
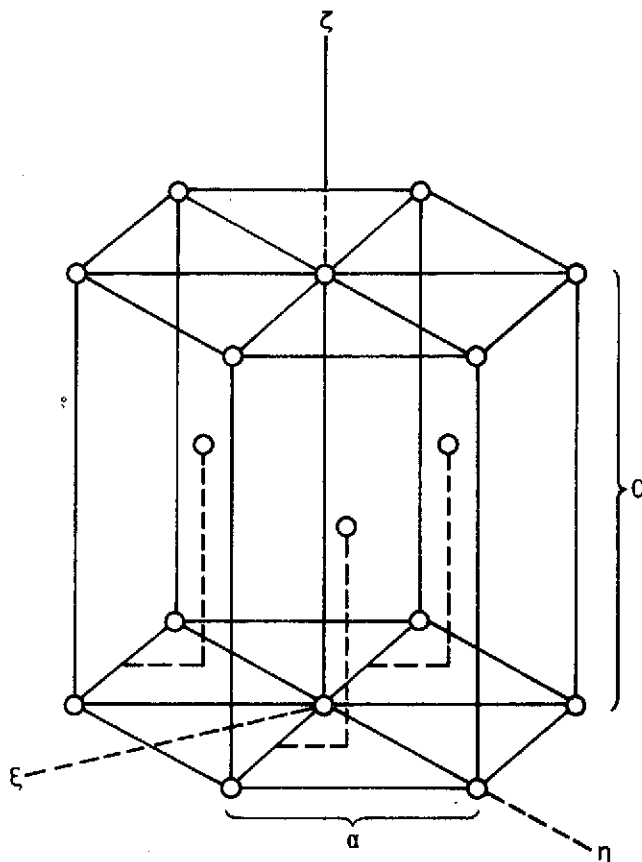
Figure 1. - Hexagonal-close-packed (hcp) structure
pertinent to heavy rare earth metals.

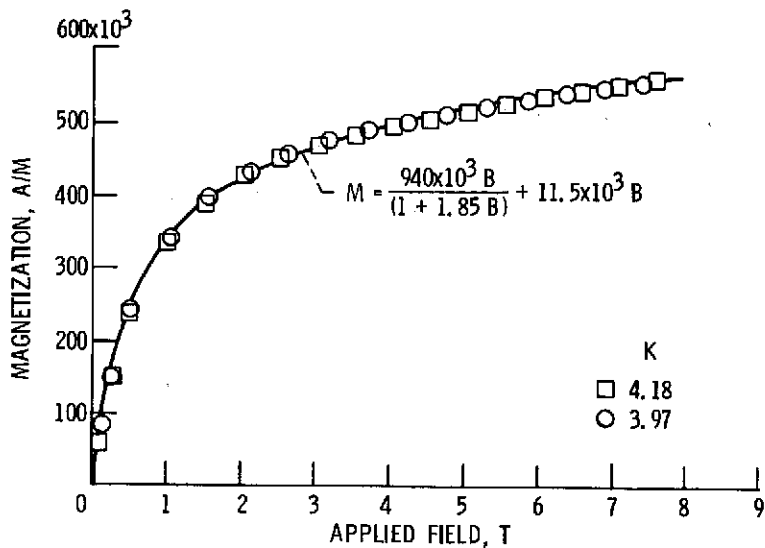$$M = \frac{940 \times 10^3 \, B}{(1 + 1.85 \, B)} + 11.5 \times 10^3 \, B$$

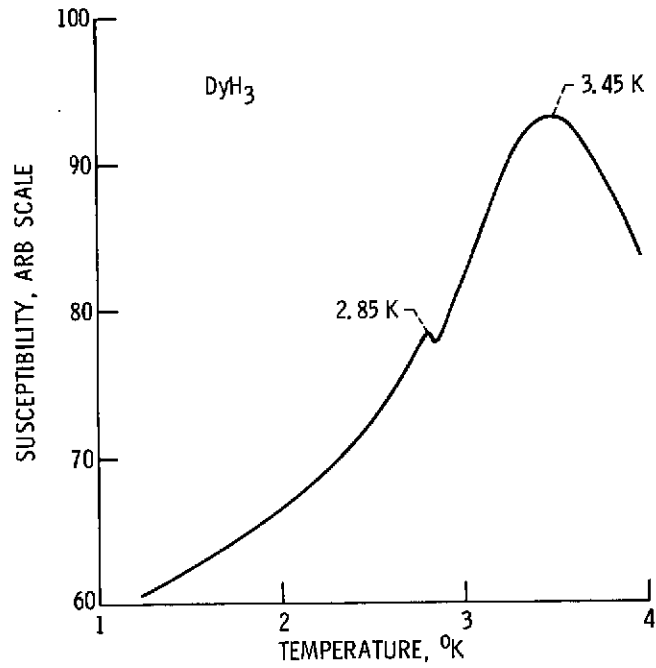Figure 2. - Magnetization versus applied magnetic field for DyH$_3$.

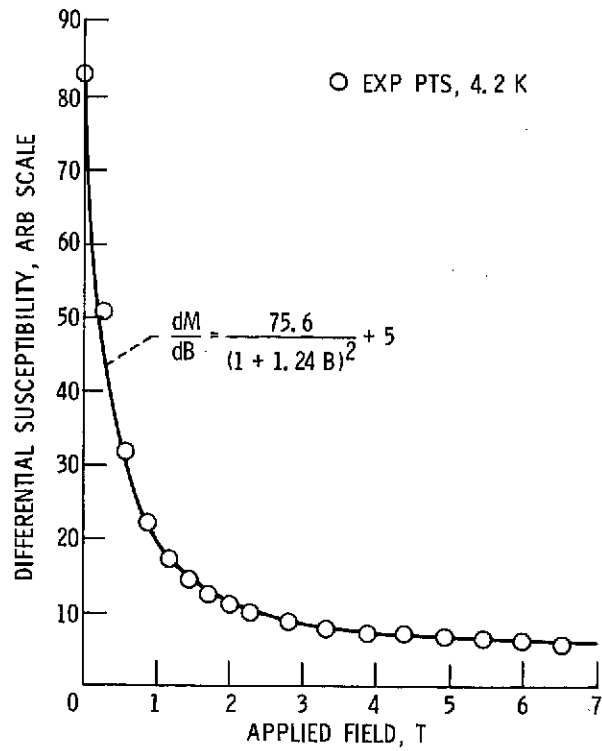Figure 3. - Magnetic susceptibility versus temperature for DyH$_3$.

Figure 4. - Magnetic susceptibility versus applied magnetic field for DyH$_3$.